Somatostatin Receptor Scintigraphy with Indium-111-DTPA-D-Phe-1-Octreotide in Man: Metabolism, Dosimetry and Comparison with Iodine-123-Tyr-3-Octreotide

E.P. Krenning, W.H. Bakker, P.P.M. Kooij, W.A.P. Breeman, H.Y. Oei, M. de Jong, J.C. Reubi, T.J. Visser, C. Bruns, D.J. Kwekkeboom, A.E.M. Reijs, P.M. van Hagen, J.W. Koper, and S.W.J. Lamberts

Departments of Nuclear Medicine and Internal Medicine III, University Hospital Dijkzigt, Rotterdam, The Netherlands; Sandoz Research Institute, Berne and Department of Endocrinology, Sandoz Pharma AG, Basel, Switzerland

Scintigraphy with ^{123}I-Tyr-3-octreotide has several major drawbacks as regards its metabolic behavior, its cumbersome preparation and the short physical half-life of the radionuclide. The use of another radiolabeled analog of somatostatin, ^{111}In-DTPA-D-Phe-1-octreotide, has consequently been proposed. DTPA-D-Phe-1-octreotide can be radiolabeled with ^{111}In in an easy single-step procedure. DTPA-D-Phe-1-octreotide is cleared predominantly via the kidneys. Fecal excretion of radioactivity amounts to only a few percent of the administered radioactivity. For the radiation dose to normal tissues, the most important organs are the kidneys, the spleen, the urinary bladder, the liver and the remainder of the body. The calculated effective dose equivalent is 0.08 mSv/MBq. Optimal ^{111}In-DTPA-D-Phe-1-octreotide scintigraphic imaging of various somatostatin receptor-positive tumors was obtained 24 hr after injection. In the six patients studied, tumor localization with ^{123}I-Tyr-3-octreotide and with ^{111}In-DTPA-D-Phe-1-octreotide were found to be similar. However, the normal pituitary is more frequently visualized with the latter radiopharmaceutical. In conclusion, ^{111}In-DTPA-D-Phe-1-octreotide appears to be a sensitive somatostatin receptor-positive tissue-seeking radiopharmaceutical with some remarkable advantages: easy preparation, general availability, appropriate half-life and absence of major interference in the upper abdominal region, because of its renal clearance. Therefore, ^{111}In-DTPA-D-Phe-1-octreotide may be suitable for use in SPECT of the abdomen, which is important in the localization of small endocrine gastroenteropancreatic tumors.

J Nucl Med 1992; 33:652–658

We recently introduced the somatostatin analog Tyr-3-octreotide labeled with ^{123}I for the localization of primary and metastatic somatostatin receptor-rich tumors, such as carcinoids, islet cell tumors of the pancreas, paragangliomas and small-cell carcinomas of the lungs (*1–4*). Our experience points to several drawbacks of ^{123}I-Tyr-3-octreotide in its use for in vivo scintigraphy. First, the labeling of Tyr-3-octreotide with ^{123}I is cumbersome and requires special skills. Second, Na^{123}I of high specific activity (*5,6*) is expensive and hardly available worldwide. Third, the moment of the labeling and scanning procedures is dependent on the logistics of the production and delivery of Na^{123}I. Finally, substantial accumulation of radioactivity is seen in the intestines, since a major part of ^{123}I-Tyr-3-octreotide is rapidly cleared via the liver and biliary system. This makes the interpretation of planar and single-photon emission computed tomographic (SPECT) images of the upper abdomen difficult.

Part of these problems can be solved by replacing ^{123}I with ^{111}In, which also improves scintigraphy 24–48 hr after application by virtue of its longer half-life. Binding of ^{111}In to the somatostatin analog octreotide has been carried out by complexing with a diethylenetriaminepentaacetic acid (DTPA) group coupled to the αNH_2-group of the N-terminal D-Phe residue (*7*). In rats, it appeared that ^{111}In-DTPA-D-Phe-1-octreotide: (1) is excreted via the kidneys, (2) shows only minor accumulation in the liver and (3) has an initial plasma half-life in the order of minutes (*8*).

In this study, we report data concerning the metabolism of intravenously administered ^{111}In-DTPA-D-Phe-1-octreotide in man, as well as estimates of its radiation dose in principal organs and the effective dose equivalent. Also, scintigraphic images of various somatostatin receptor-positive tumors have been compared using both ^{123}I-Tyr-3-octreotide and ^{111}In-DTPA-D-Phe-1-octreotide as radiopharmaceuticals in the same patients.

MATERIALS AND METHODS

Radiopharmaceuticals

The somatostatin derivatives DTPA-D-Phe-1-octreotide (SDZ 215-811) and Tyr-3-octreotide (SDZ 204-090) were prepared by

Received Jul. 23, 1991; revision accepted Dec. 4, 1991.

For reprints contact: E. P. Krenning, MD, PhD, Professor of Nuclear Medicine, University Hospital Dijkzigt, Department of Nuclear Medicine, Dr Molewaterplein 40, 3015 GD Rotterdam, The Netherlands.

Sandoz (Basel, Switzerland). Indium-111-chloride ("ultra-pure") and Na^{123}I were obtained from Mallinckrodt Diagnostica (Petten, The Netherlands) and Medgenix (Fleurus, Belgium), respectively. Indium-111-chloride contained ^{114m}In to a limited extent (0.5 kBq ^{114}In/MBq ^{111}In at calibration time). Radiolabeling of DTPA-D-Phe-1-octreotide with ^{111}In and of Tyr-3-octreotide with ^{123}I and quality control of the products were performed as described before (*5–8*). Depending on the interval between injection and scintigraphy, and whether SPECT was required, the administered radioactivity of ^{111}In-DTPA-D-Phe-1-octreotide and of ^{123}I-Tyr-3-octreotide ranged from 185 to 259 MBq and from 370 to 555 MBq, respectively, given as an intravenous bolus. The administered dose of the somatostatin analogs varied from 7 to 20 μg per injection.

Imaging

Planar and SPECT images were obtained with a large field of view gamma camera (Counterbalance 3700 and ROTA II, Siemens, Hoffman Estates, IL), equipped with a medium-energy parallel-hole collimator. The pulse-height analyzer windows were centered over both ^{111}In photon peaks (172 keV and 245 keV) with a window width of 20%. Data from both windows were added to the acquisition frames. The camera was connected to a dedicated PDP 11/73 computer (Digital Equipment Corp., Maynard, MA) using the Gamma 11 and SPETS V 6.1 software (Nuclear Diagnostics, Stockholm, Sweden). The acquisition parameters for planar images were: (1) 128 × 128 word matrix, (2) images of head/neck: 300,000 preset counts (or max. 15 min) at 24 hr and 15 min preset time (≈200,000 counts) at 48 hr after injection and (3) images of the rest of the body: 500,000 counts (or max. 15 min); for SPECT: (1) 60 projections, (2) 64 × 64 word matrix and (3) 60-sec acquisition time per projection. SPECT analysis was performed with a Wiener filter on original data. The filtered data were reconstructed with a ramp filter. If indicated, SPECT studies were performed 4 hr (head and neck) or 24 hr (remainder of the body) after injection of the radiopharmaceutical. Planar studies were carried out both after 24 hr and 48 hr (vide supra), and in a few cases also after 0.5 hr and 4 hr with the same protocol used in the 24-hr studies. Total-body scintigraphy (scintigraphy of extremities only if indicated) of every patient was performed at least once, usually 24 hr after injection.

Measurement of ^{111}In Radioactivity in Blood, Urine and Feces

Radioactivity in blood, urine and feces was measured with an LKB-1282-Compugamma system or a GeLi-detector equipped with a multi-channel analyser (Series 40, Canberra).

Blood samples were collected directly before injection and 2, 5, 10, 20 and 40 min and 1, 4, 20 and 48 hr after injection. Urine was collected from the time of injection in two 3-hr intervals and thereafter in intervals of 6 hr until 48 hr after injection. If feasible, feces was collected until 72 hr after injection. The chemical status of the radionuclide in blood and urine was analyzed as a function of time by using the SEP-PAK C18, HPLC and gel filtration techniques as described previously (*5*). The nature of peptide-bound radioactivity in blood and urine was tested by investigation of specific binding to somatostatin receptors on rat brain cortex cell membranes as described previously (*9*).

Patients

The data described in this paper were derived from patients who had been referred for a variety of potentially somatostatin receptor-positive tumors. All patients gave informed consent to participate in the study, which had been approved by the ethics committee of our hospital. Kinetic studies with ^{111}In-DTPA-D-Phe-1-octreotide by means of gamma camera scintigraphy were performed in 26 patients. Additionally, plasma, urine and feces samples were obtained from 9, 10, and 4 patients, respectively. In another six patients we were able to perform somatostatin-analog scintigraphy with ^{123}I-Tyr-3-octreotide as well as with ^{111}In-DTPA-D-Phe-1-octreotide with a maximum interval of 3 mo.

Dosimetry

For the estimation of the radiation dose, the MIRDOSE version 2 program (*10*) and ICRP publication 53 (*11*) were used. The uptakes in the most important source organs, the kidneys, the spleen, the liver, the urinary bladder and the remainder of the body, were determined as a function of time. Radioactivity in the kidneys, liver and spleen was calculated as described before (*6*). Radioactivity in the urinary bladder was calculated using the measured radioactivity excreted in the urine and assuming a bladder voiding interval of 3.5 hr (*11*). Radioactivity in the remainder of the body (expressed as percentage of the administered radioactivity) as a function of time was determined as 100% minus the % uptake in kidneys, liver, spleen, urinary bladder and excreted radioactivity in urine and feces.

In eight patients, the uptake in the kidneys, spleen and liver was measured with the gamma camera 0.5, 4, 24 and 48 hr after injection of ^{111}In-DTPA-D-Phe-1-octreotide. The results obtained in two patients could not be used because of an extensive overlap of the right kidney and the liver. In the six remaining patients, the excreted radioactivity in the urine (until 48 hr after ^{111}In-DTPA-D-Phe-1-octreotide injection) was measured as well. In four patients, the fecal excretion was also determined until 72 hr after injection. The calculation of the radiation dose in the gastrointestinal tract was performed using the mean radioactivity detected in the feces of these four patients. The dose estimates of the various organs and the effective dose equivalent were calculated for each of the six patients individually.

In order to perform dosimetry when only gamma camera measurements were available 24 and 48 hr after ^{111}In-DTPA-D-Phe-1-octreotide injection, a model was developed. In this model the residence times for the kidneys, spleen and liver were calculated for each individual patient on the basis of the organ uptakes after 24 and 48 hr. For the urinary bladder contents and the remainder of the body measurements, mean residence times were used. With this model, it was possible to calculate the dose estimates and the effective dose equivalent in another 18 patients. Apart from the organs mentioned above, radioactivity was seen in both the thyroid and pituitary glands in most patients.

RESULTS

Metabolism

The average plasma radioactivity decreased rapidly after injection of ^{111}In-DTPA-D-Phe-1-octreotide in nine patients. Assuming a plasma volume of 3 liters, the mean radioactivity in the blood circulation was calculated to decrease within 10 min to 33% ± 7% (s.d.) of the injected

amount. In five patients, the chemical status of the radionuclide in the plasma was investigated as a function of time. In Figure 1, the time course of total and peptide-bound radioactivity in the plasma of these five patients are presented up to 20 hr after injection of ^{111}In-DTPA-D-Phe-1-octreotide. During the first 4 hr, plasma radioactivity was mainly peptide-bound in the form of intact ^{111}In-DTPA-D-Phe-1-octreotide as demonstrated by HPLC. Only the last two points of the observation period showed proportionally increasing amounts of non-peptide-bound radioactivity, eluting in the void volume.

Urinary excretion of radioactivity was measured in ten patients. In five of these patients, the chemical status of the radionuclide in the urine was also investigated. Figure 2 shows the rapid excretion of the administered radioactivity via the urine from about 25% after 3 hr, 50% after 6 hr, 85% after 24 hr to over 90% after 48 hr for this group of five patients. Figure 2 also shows that the excreted radioactivity was mainly peptide-bound in these patients. SEP-PAK and HPLC analyses of urine and plasma samples as functions of time after injection demonstrated that peptide-bound radioactivity predominantly consisted of ^{111}In-DTPA-D-Phe-1-octreotide during the first hours after injection. Twenty-four hours after injection, in addition to ^{111}In-D-Phe-1-octreotide and peptide-bound degradation products, a major part of urinary radioactivity eluted from the HPLC in the void volume (Fig. 3). Feces, collected until 72 hr after injection of ^{111}In-DTPA-D-Phe-1-octreotide from four patients with normal intestinal function, contained less than 2% of the administered radioactivity. The SEP-PAK C18 and HPLC-purified radiolabeled peptide component in plasma and urine showed the same biological activity as the radiopharmaceutical itself, as indicated by its specific binding to somatostatin receptors on rat brain cortex cell membranes (data not shown).

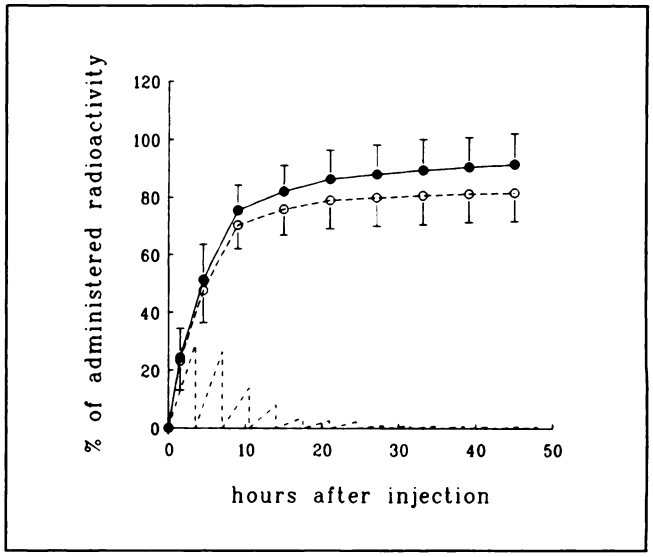

FIGURE 2. Cumulative total (·) and peptide-bound (O) ^{111}In urinary excretion (n = 5) and mean urinary bladder radioactivity voiding (—) (n = 5) after intravenous injection of ^{111}In-DTPA-D-Phe-1-octreotide. Data are expressed as mean ± s.d. percentage of the administered radioactivity.

Dosimetry

The uptake of radioactivity in the liver, spleen and kidneys was measured with the gamma camera in six patients. If either the thyroid or the pituitary, or both, were clearly distinguishable from the surrounding tissue, the uptake in these organs was measured as well. Other organs (e.g., the intestines) showed low accumulation of radioactivity and were, therefore, disregarded in the gamma cam-

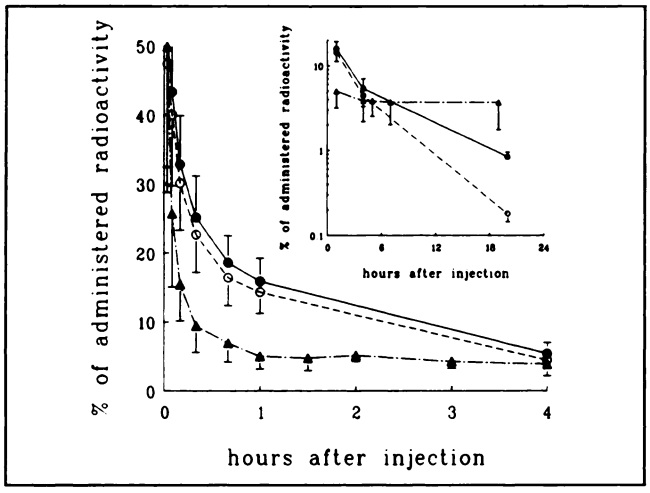

FIGURE 1. Total plasma (·) and peptide-bound (O) radioactivity after administration of ^{111}In-DTPA-D-Phe-1-octreotide in five patients. Results are compared with total plasma (▲) radioactivity after administration of ^{123}I-Tyr-3-octreotide in seven patients taken from reference 6. Data are expressed as mean ± s.d. percentage of the administered radioactivity. Note the logarithmic scale of values in the ordinate of the inset.

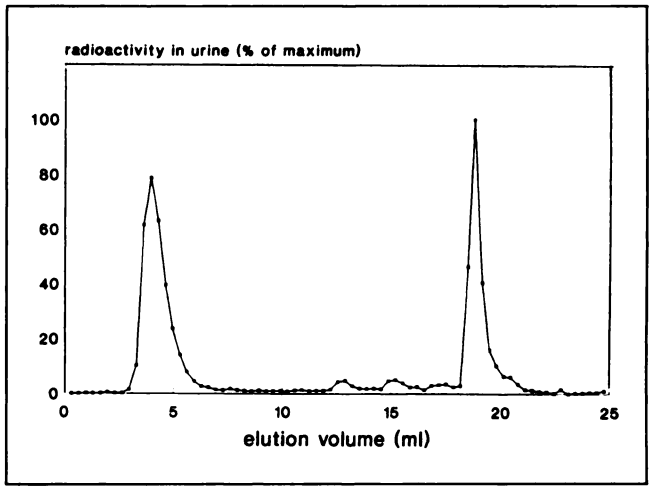

FIGURE 3. Typical HPLC-elution profile of human urine, collected 24 hr after intravenous injection of ^{111}In-DTPA-D-Phe-1-octreotide. At a retention volume of about 4 ml, non-peptide-bound ^{111}In, such as ^{111}In-DTPA, is eluted at 12–18 ml ^{111}In containing degradation products and at about 19 ml the original radioligand.

era measurements. The time courses of radioactivity in the liver, spleen and kidneys showed close similarities between individual patients (data not shown). The results of the uptake measurements are given in Table 1. Five thyroid and two pituitaries in the group of six patients could be completely distinguished from the surrounding background (vide infra). The radioactivity in the thyroid (maximal 0.03%) and the pituitary (maximal 0.003%) varied strongly between individual patients. Frequently, these organs were only visible on the 24-hr images. Therefore, the residence time was calculated assuming that the effective half-life equals the physical half-life. The absorbed doses for the thyroid and the pituitary (*12,13*), corresponding to the maximum uptake measured in the group of six patients, are given in Table 2. Radioactivity excreted in the urine was used for calculation of the residence time of the urinary bladder contents for all patients and showed the same course as the mean depicted in Figure 2. For all patients, the radioactivity in the feces was taken to be the mean of the radioactivity measured in the four patients (0.5% and 1.7% after 24 and 48 hr, respectively). Even assuming that these maximum values occurred in the same patient, the contribution of the thyroid, the pituitary and the feces to the effective dose equivalent was less than 5% and could therefore be neglected. The dose estimates of the various organs and the effective dose equivalent were calculated for these six patients (data not shown).

The contribution to the absorbed dose caused by the ^{114m}In contamination was calculated on the basis of the information obtained from the manufacturer and was found to be less than 0.5% of the dose from ^{111}In. In practice, the radionuclide was administered before the calibration time, thus lowering even more the contribution of ^{114m}In to the radiation dose.

TABLE 1
Radioactivity in Selected Organs and Remainder of the Body (mean ± s.d.) as a Function of Time After Intravenous Administration of ^{111}In-DTPA-D-Phe1-Octreotide in Man on the Basis of Gamma Camera Measurements and Calculations Expressed as Percentage of the Administered Radioactivity

Time (hr)	n	%Uptake Liver	Spleen	Kidneys	Remainder of the body*
0.5	6	2.8 ± 1.2	2.0 ± 0.9	6.8 ± 1.3	84.2 ± 7.7
4	6	1.9 ± 0.4	2.4 ± 0.9	7.2 ± 1.8	46.7 ± 17.9
24	6	2.2 ± 0.6	2.6 ± 1.1	6.3 ± 2.1	8.7 ± 9.7
48	6	1.8 ± 0.4	1.8 ± 0.6	5.0 ± 2.0	7.2 ± 8.8
24	18	3.0 ± 1.3	2.9 ± 1.6	4.8 ± 1.7	
48	18	2.5 ± 1.0	2.1 ± 1.2	3.5 ± 1.3	

* The radioactivity in the remainder of the body is the administered radioactivity (100%) minus the %radioactivity in liver, spleen, kidneys, urinary bladder, urine and feces.

TABLE 2
Dose Estimates After Intravenous Administration of ^{111}In-DTPA-D-Phe-1-Octreotide in Man on the Basis of Gamma Camera Measurements (n = 24), Urinary Excretion Measurements (n = 10) and Fecal Excretion Measurements (n = 4).

Target organ	Absorbed dose (mGy/MBq)	Range (mGy/MBq)
Kidneys	0.45^{MD}	0.19–0.80
Liver	0.07^{MD}	0.04–0.15
Spleen	0.32^{MD}	0.10–0.66
Gonads	0.019^{MD}	0.015–0.026
Red marrow	0.020^{MD}	0.016–0.026
Urinary bladder wall	0.18^{MN}	n.a.*
GI tract		
Small intestinal wall	$0.03^{MN,\dagger}$	n.a.*
ULI wall	$0.04^{MN,\dagger}$	n.a.*
LLI wall	$0.06^{MN,\dagger}$	n.a.*
Thyroid gland	0.04^{MX}	
Pituitary	0.11^{MX}	

Median effective dose equivalent (mSv/MBq)	Range (mSv/MBq)
0.08	0.05–0.12

The input to the small intestines is taken to be the same as the fecal excretion during 72 hr (n = 4), viz 1.7%. For the thyroid and the pituitary (n = 6), the radiation dose corresponds to the maximum organ uptake measured in these patients.

^{MD} denotes median.

^{MN} denotes mean.

^{MX} denotes calculations for maximum uptake.

* Not applicable due to the model.

† ICRP 30 GI model used.

On the basis of the data obtained in the six patients, it appears that more than 70% of the effective dose equivalent results from radioactivity accumulated in the kidneys, spleen and liver. The uptake of radioactivity in these organs showed much greater individual variation in these six patients than the radioactivity excreted in the urine and the calculated uptake in the remainder of the body. Therefore, in the model employed, the uptake of radioactivity in the liver, kidneys and spleen is based on individual gamma camera measurements. Table 1 shows that in the group of six patients, radioactivity in the spleen increases slightly from 0.5 to 24 hr and decreases afterwards in all patients. In the liver, the radioactivity decreases rapidly during the first hour, thereafter an increase is measured until 24 hr, followed by a decrease. For the calculation of the residence time in the model, the radioactivity in the liver and the spleen was assumed to remain constant from 0 to 24 hr and to decrease after 24 hr monoexponentially with time. Radioactivity in the kidneys shows a steady decrease (Table 1) starting shortly after the injection of the radiopharmaceutical. For this reason, the calculation of the kidney residence time was based on a monoexponential curve. The initial uptake in the kidneys was calculated by extrapolating the uptakes at 24 and 48 hr to t = 0.

The periodic accumulation and discharge of radioactivity in the urinary bladder was calculated from the mean

collected urinary radioactivity in 10 patients. There is no significant difference in the cumulative urinary radioactivity between these 10 patients and the 5 patients presented in Figure 2. The radioactivity in the remainder of the body was calculated by subtraction of the mean uptakes in the kidneys (n = 6), spleen (n = 6), liver (n = 6), urinary bladder contents (n = 10) and mean excreted radioactivity in urine (n = 10) and feces (n = 4) from the administered amount. The residence time in the remainder of the body could be determined by fitting a monoexponential curve to the radioactivity course after injection. The six patients were recalculated using the model described. There were no statistically significant differences in the dose estimates of the various organs and in the effective dose equivalent in comparison to the direct estimates for each individual (data not shown). Therefore, application of the model appeared to be valid. In 18 patients, the uptake in the kidneys, spleen and liver was measured after 24 and 48 hr (Table 1). These data did not differ significantly from the values obtained at the same time points in the six patients. Consequently, the model was applied to the additional 18 patients. The final dosimetric results for the complete group of 24 patients are shown in Table 2.

Iodine-123-Tyr-3-Octreotide and ^{111}In-DTPA-D-Phe-1-Octreotide Scintigraphy: Comparison in Localization of Tumor Tissue

A comparison between scintigraphy with ^{123}I-Tyr-3-octreotide and scintigraphy with ^{111}In-DTPA-D-Phe-1-octreotide, performed in an interval of less than 3 mo for the same patients, is given in Table 3. In four of six patients (Patients 1–3, and 6) the results of the subsequent scintigrams were identical. In Patient 2, ^{123}I-Tyr-3-octreotide scintigraphy showed accumulation of radioactivity in the region of the gallbladder, which is not unusual for this radiopharmaceutical, considering its extensive biliary clearance. However, the same was observed with ^{111}In-DTPA-D-Phe-1-octreotide, which is unusual, since this radiopharmaceutical is largely excreted by the kidneys. SPECT with ^{111}In-DTPA-D-Phe-1-octreotide demonstrated a tumor located ventral to the gallbladder. In Patient 3, SPECT images after ^{111}In-DTPA-D-Phe-1-octreotide injection revealed the localization of the insulinoma, medial and anterior to the spleen and left kidney respectively (Fig. 4). However, this localization had not been recognized on planar images with both radiopharmaceuticals. In Patient 4, presumed carcinoid deposits were more numerous using ^{111}In-DTPA-D-Phe-1-octreotide scintigraphy. Tumor progression in the relatively long interval between the two scintigrams cannot be excluded, however. In Patient 5, the liver showed an irregular uptake pattern of ^{111}In-DTPA-D-Phe-1-octreotide, whereas a homogeneous distribution was seen with ^{123}I-Tyr^3-3-octreotide scintigraphy. The cranial abdominal site of radionuclide accumulation observed with ^{123}I-Tyr-3-octreotide was not seen on the subsequent ^{111}In-DTPA-D-Phe-1-octreotide scintigram. This site very likely represented abnormal uptake in the gallbladder and the hepatoduodenal ligament, which had been surgically removed between the two scintigrams and were proven to be massively infiltrated by a carcinoid tumor.

Apart from the marked differences in hepatic and renal clearances (Fig. 5), tissue accumulation of both radiopharmaceuticals was similar except for the pituitary, which was nearly always visible with ^{111}In-DTPA-D-Phe-1-octreotide in contrast to ^{123}I-Tyr-3-octreotide scintigraphy. However, discrimination between accumulation of ^{111}In-DTPA-D-Phe-1-octreotide in the pituitary and in the surrounding tissues is often impossible, especially caudally. Consequently, only the contour of the cranial part of the pituitary can be distinguished since in the region of the brain the (background) radioactivity is relatively very low because of the blood-brain barrier. For both radiopharmaceuticals, radioactivity was always observed in the thyroid, liver, spleen and kidneys, the urinary bladder and in the intestinal tract, although in the last organ ^{111}In-DTPA-D-Phe-1-octreotide was much less visible.

DISCUSSION

In spite of a lower affinity of ^{111}In-DTPA-D-Phe-1-octreotide for the rat brain somatostatin receptor com-

TABLE 3
Patient Data and Results of Somatostatin-Receptor Scintigraphy with ^{123}I-Tyr-3-Octreotide and ^{111}In-DTPA-D-Phe-1-Octreotide

Patient no.	Sex	Age	Tumor type	Interval between scans	Abnormal sites of radioactive accumulation	
					^{123}I-octreotide	^{111}In-octreotide
1	F	66	Small-cell lung cancer	5 wk	Right lung, lower lobe	Right lung, lower lobe
2	M	65	Gastrinoma	7 wk	Gallbladder region	Gallbladder region (see text)
3	F	59	Insulinoma	1 wk	None (SPECT not done)	None (SPECT positive, Fig. 4)
4	F	50	Carcinoid	10 wk	Left supraclavicular lymph node, liver	Left+right supraclavicular lymph node, abdomen, chest, liver
5	F	64	Carcinoid	5 wk	3 caudal abdominal sites, 1 cranial abdominal site	3 caudal abdominal sites, liver (gallbladder removed; see text)
6	F	28	Pheochromocytoma	4 wk	Lower left abdomen	Lower left abdomen

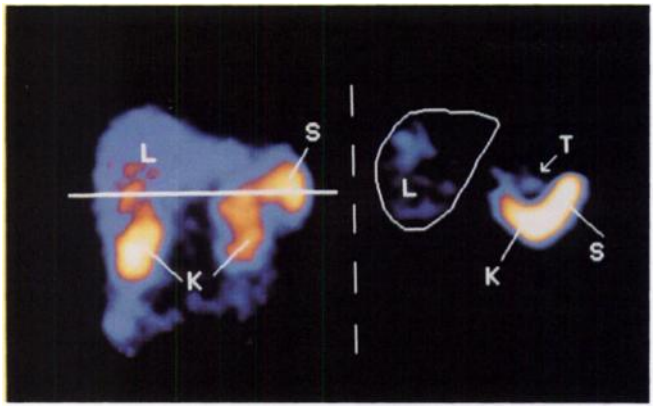

FIGURE 4. Indium-111-DTPA-D-Phe-1-octreotide 24 hr SPECT image of Patient 3 with a solitary insulinoma in the tail of the pancreas, which is shown medial and anterior to the spleen and left kidney. The line on the reference image (left) indicates the position of the transversal slice (right). K = kidney, S = spleen, T = tumor and L = liver.

pared to that of ^{123}I-Tyr-3-octreotide (*7*), the indium-labeled compound visualized somatostatin receptor-positive animal tumors more efficiently in vivo, probably due to its different metabolic behavior (*8*). These metabolic properties turned out to be similar in man; our study shows that after intravenous administration ^{111}In-DTPA-D-Phe-1-octreotide is rapidly cleared from the circulation via the kidneys. However, its initial disappearance from the circulation is considerably slower compared to that of ^{123}I-Tyr-3-octreotide (Fig. 1) (*6*). This slower initial clearance, combined with the longer physical half-life of ^{111}In

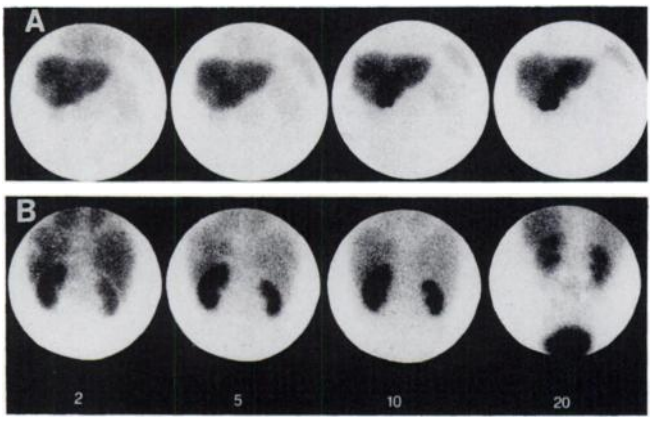

FIGURE 5. Sequential anterior abdominal views of ^{123}I-Tyr-3-octreotide scintigraphy (A) showing rapid hepatobiliary clearance, and posterior abdominal views of ^{111}In-DTPA-D-Phe-1-octreotide scintigraphy (B) showing rapid renal clearance. Note the rapidly decreasing blood-pool radioactivity over the heart with both radiopharmaceuticals. The 20-min image of the latter scintigrams also shows a low-grade accumulation of radioactivity in the lower part of the vertebral column due to a chondrosarcoma.

($t_{1/2}$ = 2.8 days for ^{111}In versus 13.2 hr for ^{123}I) results in a longer residence time of the radiopharmaceutical in the tissues. The presence of a lower radioactivity in the remainder of the body 24 hr after injection of ^{111}In-DTPA-D-Phe-1-octreotide leads to a lower background radioactivity (Fig. 1) (*6*). The higher background radioactivity with ^{123}I-Tyr-3-octreotide is due to its much higher circulating levels of degradation products than is the case with ^{111}In-DTPA-D-Phe-1-octreotide. Therefore, ^{111}In-DTPA-D-Phe-1-octreotide is a more suitable radioligand to localize somatostatin receptor-rich tissues (vide infra). Furthermore, using ^{111}In-DTPA-D-Phe-1-octreotide, interpretation of scintigrams of the abdominal region is less affected by intestinal background radioactivity. This contrasts remarkably with ^{123}I-Tyr-3-octreotide scintigraphy, because the hepatobiliary clearance of this compound results in a high hepatic and intestinal accumulation of radioactivity, which is hardly overcome with laxatives.

Analysis of the chemical status of plasma radioactivity during the first 4 hr after injection shows mainly peptide-bound ^{111}In in the form of the original ^{111}In-DTPA-D-Phe-1-octreotide. Similarly, analysis of radioactivity in the urine shows predominantly intact ^{111}In-DTPA-D-Phe-1-octreotide during the first hours after injection. Furthermore, peptide-bound radioactivity in plasma and urine has somatostatin receptor-binding properties as demonstrated by specific binding to rat brain cortex cell membranes. Degradation of ^{111}In-DTPA-D-Phe-1-octreotide was observed only in plasma and urine samples obtained more than 4 hr after intravenous injection of the radiopharmaceutical, when circulating radioactivity amounted to less than 10% of the administered radioactivity. Ultimately, degradation to ^{111}In-labeled products such as ^{111}In-DTPA is suggested by the appearance of the peak in the void volume of HPLC analysis.

Accumulation of radioactivity after intravenous administration of ^{111}In-DTPA-D-Phe-1-octreotide in man is observed in the pituitary and thyroid gland, the spleen, liver, kidneys and the urinary bladder. Imaging of the gallbladder is occasionally seen, whereas the presence of intestinal radioactivity (mainly in the colon at 24 hr) depends on the simultaneous use of laxatives. The relatively low clearance of the radioligand via the hepatobiliary system favors its use in SPECT of the abdomen, which is strongly indicated in the localization of small endocrine pancreatic tumors. The mechanism of the thyroid gland imaging is still unclear. With radiolabeled somatostatin analogue autoradiography, we could not find somatostatin receptors in normal thyroid gland and differentiated thyroid carcinoma (papillary cancer) tissue slices (*14,15*). However, a high percentage of malignant parafollicular thyroid tumors are somatostatin receptor-positive by both autoradiography and scintigraphy (*14,15*). It is remarkable that in the two cases with Graves' hyperthyroidism investigated so far, accumulation of radioactivity in the thyroid was increased (unpublished data). The presence of lymphocytes

[which can be somatostatin receptor-positive (*16*)] in the thyroid could explain this observation. Autoradiography of normal spleen tissue revealed the presence of somatostatin receptors (unpublished); however, the exact cell type bearing the somatostatin receptor has not been identified yet. Patients on octreotide treatment show a diminished accumulation of radioligand in the spleen (unpublished), compatible with occupancy of spleen somatostatin receptors by the unlabeled octreotide.

The rapid appearance of intact ^{111}In-DTPA-D-Phe-1-octreotide in the urine indicates an effective renal clearance of this radiopharmaceutical. By contrast, ^{123}I-Tyr-3-octreotide is rapidly cleared by the liver and little of it is excreted intact into the urine. The different metabolism of ^{111}In-DTPA-D-Phe-1-octreotide compared with ^{123}I-Tyr-3-octreotide indicates that the modification of octreotide with the ^{111}In-DTPA group inhibits hepatic clearance and/or facilitates renal clearance. Rat liver perfusion studies have indeed shown that ^{111}In-DTPA-D-Phe-1-octreotide is cleared much more slowly by the liver than ^{123}I-Tyr-3-octreotide (unpublished data). It is unknown whether the effect of the ^{111}In-DTPA group on the metabolic routing of peptides is a general phenomenon. The relatively long residence time of ^{111}In-DTPA-D-Phe-1-octreotide in the kidneys suggests that following glomerular filtration part of the label is reabsorbed in the tubules (*8*).

The higher sensitivity of ^{111}In-DTPA-D-Phe-1-octreotide compared to ^{123}I-Tyr-3-octreotide in localizing the pituitary is remarkable, since in vitro studies have shown a higher affinity of the radioiodinated ligand for somatostatin receptors in rat brain (*7*). However, its actual affinity for somatostatin receptors on the pituitary is at present unknown.

For several somatostatin receptor-positive tumors, ^{111}In-DTPA-D-Phe-1-octreotide shares with ^{123}I-Tyr-3-octreotide the advantage of providing a more sensitive imaging technique when compared to currently available diagnostic procedures, e.g., CT, ultrasound and MRI. Furthermore, the future availability of both DTPA-D-Phe-1-octreotide and pure $^{111}InCl_3$, will make an easy single-step labeling procedure possible and, hence, scintigraphy of somatostatin receptor-positive tumors generally available. The effective dose equivalent, although higher than that of ^{123}I-Tyr-3-octreotide, is comparable with values for other ^{111}In-labeled radiopharmaceuticals (*11*) and is acceptable in view of the clinical indications.

ACKNOWLEDGMENTS

The authors thank Ina Loeve, Marianne Goemaat-Visser, Marcel van der Pluijm and Michiel de Roo for their expert technical assistance and Michael Stabin for providing the S-value tables for ^{114m}In.

REFERENCES

1. Krenning EP, Bakker WH, Breeman WAP, et al. Localisation of endocrine-related tumours with radioiodinated analogue of somatostatin. *Lancet* 1989;1:242–244.
2. Lamberts SWJ, Bakker WH, Reubi J-C, Krenning EP. Somatostatin-receptor imaging in the localization of endocrine tumors. *N Engl J Med* 1990;323:1246–1249.
3. Lamberts SWJ, Hofland LJ, van Koetsveld PM, et al. Parallel in vivo and in vitro detection of functional somatostatin receptors in human endocrine pancreatic tumors: consequences with regard to diagnosis, localization, and therapy. *J Clin Endocrinol Metab* 1990;71:566–574.
4. Kwekkeboom DJ, Krenning EP, Bakker WH, et al. Radioiodinated somatostatin analog scintigraphy in small-cell lung cancer. *J Nucl Med* 1991; 32:1845–1848.
5. Bakker WH, Krenning EP, Breeman WAP, et al. Receptor scintigraphy with a radioiodinated somatostatin analogue: radiolabeling, purification, biologic activity and in vivo application in animals. *J Nucl Med* 1990;31: 1501–1509.
6. Bakker WH, Krenning EP, Breeman WAP, et al. In vivo use of a radioiodinated somatostatin analogue: dynamics, metabolism and binding to somatostatin receptor positive tumors in man. *J Nucl Med* 1991;32: 1184–1189.
7. Bakker WH, Albert R, Bruns C, et al. [^{111}In-DTPA-D-Phe^1]-octreotide, a potential radiopharmaceutical for imaging of somatostatin receptor-positive tumors: synthesis, radiolabeling and in vitro validation. *Life Sci* 1991; 49:1583–1591.
8. Bakker WH, Krenning EP, Reubi JC, et al. In vivo application of [^{111}In-DTPA-D-Phe^1]-octreotide for detection of somatostatin receptor-positive tumors in rats. *Life Sci* 1991;49:1593–1601.
9. Reubi JC, Maurer R, Klijn JGM, et al. High incidence of somatostatin receptors in human meningiomas: biochemical characterization. *J Clin Endocrinol Metab* 1986;63:433–438.
10. Watson EE, Stabin M, Bolch WE. Documentation package for MIRDOSE (version 2). 1988, Oak Ridge Associated Universities.
11. International Commission on Radiological Protection. *Radiation dose to patients from radiopharmaceuticals.* ICRP Publication 53, Oxford: Pergamon Press; 1988.
12. Siegel JA, Stabin MG. Absorbed fractions for electrons and bèta particles in small spheres [Abstract]. *J Nucl Med* 1988;29:803.
13. Ellett WH, Humes RM. Absorbed fractions for small volumes containing photon-emitting radioactivity. MIRD Pamphlet NO. 8. *J Nucl Med* 1971; 12(suppl 5):25–32.
14. Reubi JC, Modgliani E, Calmettes C, et al. In vitro and in vivo identification of somatostatin receptors in medullary thyroid carcinomas, pheochromocytomas and paragangliomas. In: Calmettes C, Guliana JM, eds. *Medullary thyroid carcinoma.* Colloque INSERM/John Libey Eurotext Ltd.; 1991;211:85–87.
15. Reubi JC, Chayvialle JA, Franc B, et al. Somatostatin receptors and somatostatin content in medullary thyroid carcinomas. *Lab Invest* 1991; 64:567–573.
16. Sreedharan SP, Kodama KT, Peterson KE, Goetzl EJ. Distinct subsets of somatostatin receptors on cultured human lymphocytes. *J Biol Chem* 1989; 264:949–953.